COMPUTER AIDED OPTIMIZATION OF SPECIMEN GEOMETRY OF HOT TORSION TEST TO MINIMIZE MICROSTRUCTURE NON HOMOGENEITY AND TEMPERATURE GRADIENT BEFORE DEFORMATION

B. Mirzakhani[1], H. Arabi[1], M. T. Salehi[2], S. H. Seyedein[2], M. R. Aboutalebi[1], Sh. Khoddam[3] and A. Mohammadi[4]

bmirzakhani@iust.ac.ir

Received: December 2008 **Accepted: June 2009**

[1] Center of Exellence Advanced Materials and proccessing, School of metallurgy and Materials Engineering, Iran University of Science and Technology, Tehran, Iran.

[2] School of Metallurgy and Materials Engineering, Iran University of Science and Technology, Tehran, Iran.

[3] Mechanical Engineering Department, Monash University, Clayton Campus, Vic 3800, Australia.

[4] Advanced Materials Research Institute, Tehran, Iran.

Abstract: *Optimization of specimen geometry before subjecting it to hot torsion test (HTT) is essential for minimizing non-uniform temperature distribution and obtaining uniform microstructure thought the specimen.*

In the present study, a nonlinear transient analysis was performed for a number of different geometries and temperatures using the commercial finite element (FE) package ANSYSTM. FE thermal results then were applied to optimize HTT specimen produced from API-X 70 microalloyed steel taking into account the microstructure homogeneity. The thermodynamic software Thermo-calcTM was also used to analysis solubility of microalloying elements and their precipitates that may exist at different equilibrium conditions. In addition the behavior of austenite grain size during reheating was investigated. The results show high temperature gradient occurred in long specimens. This could lead to non homogeneous initial austenite grain size and alloying element or precipitates within the gauge section of the specimen. The proposed optimization procedure can in general be used for other materials and reheating scenarios to reduce temperature. This then creates more homogeneous initial microstructure prior to deformation and reduces errors in post processing of the HTT results

Keywords: *Hot torsion test, temperature gradient, Geometry optimization, Simulation, Microalloyed steel*

1. INTRODUCTION

Hot torsion test is widely used for determining the constitutive parameters for a given material [1-7]. During the hot torsion test, high strains and strain rates can be achieved without the problems of necking and barreling. The effective strain and effective stain rate in this test, depend on specimen gauge length and radius. Many researchers [1-6] have used a wide range of specimen geometries and sizes to overcome the test rig limitations in order to obtain the required strain and strain rate ranges.

Temperature measurements before and during the test can only be performed at a few points including those on the gauge surface and at the ends of the centre holes in the shoulders of the specimen. It is necessary to analyze temperature distribution and microstructure homogeneity at each stage of the HTT separately before any meaningful judgment can be made on the final errors encountered. A numerical thermo-mechanical analysis of the test at different stages namely reheating and deformation stages in conjunction with these measurements are needed to ensure uniform temperature distribution. Such procedure can only be carried out in an iterative manner to optimize the design parameters influencing temperature distribution.

The reheating treatment is the first stage of thermomechanical processes for obtaining homogeneous composition and microstructure before starting hot rolling or hot forging. The effect of austenizing temperature on initial austenite grain size and the role of microalloying elements in thermomechanical treatment of the

microalloyed steels have been investigated in several studies [6, 8-10]. These investigations show that initial microstructure has a great influence on the consequent deformation behavior of steels. Therefore, optimization of the HTT specimen geometry to provide homogeneous microstructure before starting deformation becomes a key task for an accurate process simulation.

The influences of specimen geometry of HTT and reheating conditions have not been investigated systematically. In what follows, a procedure for computer aided specimen geometry optimization will be discussed. For this purpose, the microstructure results for an API-X70 microalloyed steel in conjunction with FE thermal analyze within the HTT samples will be presented. The proposed approach is generally applicable to other materials and alloys for obtaining the optimum geometry and heating conditions before deformation. The method takes into account microstructures affected by non uniform temperature distribution.

2. COMPUTER AIDED GEOMETRY OPTIMIZATION

A wide range of geometries and specimen designs have been used in the literatures [1-7] and there exist no standard geometry in the literature. The geometry of the HTT specimen used in this research is shown in Fig. 1a.

A uniform temperature distribution within specimen may be achieved by optimizing a number of design parameters such as geometry of specimen, heating/ thermal isolation of the specimen and heating characteristics of the HTT furnace. In this investigation, the two latter parameters have been fixed and only the geometry of the test piece has been considered as the design parameter for the optimization.

For designing the HTT specimen geometry not only the thermal-mechanical study should be considered, but also microstructure homogeneity is a critical factor in order to obtain reliable final test results. In general, a sequence of thermal analysis and microstructure investigations are needed for the proposed “geometry optimization” scheme. The procedure includes the following steps:

1. Given an industrial forming process, a temperature range has to be defined according to the heating cycle performed on the material before deformation
2. The heating cycle with a similar heating cycle applied to the HTT specimen should be used. The cycle is used to model the heating during thermal FE solutions
3. Thermo-physical properties of the material should be defined.
4. Based on the required strain rate in forming process, a number of geometries have to be proposed to allow reproducing the same strain rate in the sample. The maximum and minimum angular velocity that can be accurately applied by the HTT machine should be taking into account in geometry designing.
5. For the given heating cycle, thermal FE solutions of the proposed geometries should be used.
6. Thermo-calc for investigating significant microstructure feature developments by considering temperature range predicted by the thermal simulation must be employed.
7. The history of microstructure evolution at different points of sample within the gauge section and interpretation of the results should be examined.
8. The geometries with minimum temperature gradient having the least effect on microstructure distribution as the optimum geometry of the samples must be selected.

2.1. Finite element model

Temperature distribution during reheating and before hot torsion testing was predicted in this work using the commercial FEM code ANSYS™. A two dimensional transient FE analysis of heat flow was performed to study the effect of initial heating cycle before deformation starts. The parameters are temperatures and the specimen dimensions shown schematically in Fig. 1a in order to find the sensitivity of the analysis to each dimension. The domain, boundaries and the FE mesh used are presented in Fig.1b where only one-quarter of a longitudinal

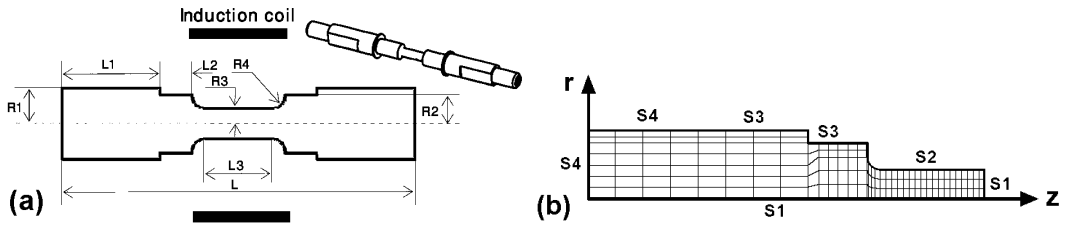

Fig. 1. a) Schematic of geometry of a solid hot torsion specimen and b) The domain and boundaries and mesh of ANSYS modeling for heating cycle before deformation

section of the specimen was considered due to the symmetry with respect to *r* and *z* axis. The analyses were conducted using at least 400 iso-parametric quadrilateral elements to ensure the accuracy of the simulation. In order to minimize the number of elements, different element sizes were used while maintaining an elemental aspect ratio of near one for the elements in the gauge section and its neighboring zones (fillets).

2.1.1. Boundary conditions

The axisymmetric conditions during reheating between the body and its environment imply that heat flux along the boundaries S1 is zero or insulated. The boundary S2 is directly heated by an induction coil of 45 mm length. The heating was controlled by a pyrometer carefully located above the middle of the specimen gauge section. The boundary S3 was exposed to the surrounding environment where the energy loss occurred through both boundary convection and radiation. A simplified approach for radiation heat transfer was utilized by using an equivalent convection boundary condition in which the non-linearity was considered through a temperature-dependent convection coefficient. The tubular quartz enclosure was applied to provide an inert atmosphere close to the specimen surface. The boundary S4 is in contact with grips of the HTT machine.

A range of HTT specimens with different gauge lengths and radii were used for optimization. They were G1(8,3.35), G2(32,3.35), G3(42,3.35), G4(52,3.35), G5(42,2.5) and G6(42,4.25). Where the values in the parentheses indicate gauge lengths and radii in mm. Specimens with long gauge length (i.e. G3, G4, G4, G5 and G6) were chosen to obtain strain rates less than 0.1 s-1. It should be noted that the hot torsion test machine considered had a minimum angular velocity of 5 rpm.

2.2. Experiment

The initial austenite grain size established at various austenizing temperatures at different points of specimen were identified experimentally for API-X70 microalloyed steel with mean chemical composition is given in Table1.

To study some microstructure features as a function of the austenitisation temperature, the thermodynamic database program Thermo-calc™ was utilized. The combination of the finite element results and the microstructure results enabled us to minimize the temperature gradient within the specimen by finding optimum geometry and reheating conditions to obtain homogenous initial microstructure.

A heating cycle was designed as shown in Fig.2 for the thermal analysis of the tests. The temperatures 740 and 860 ºC in this figure are Ac1 and Ac3 critical temperatures of present microalloyed steel respectively which were determined by dilatometry test. Low heating rate in this temperature range was considered in order to give time for transformation of ferrite and perlite to austenite. Furthermore, for validation of the predicted temperature, measurement of temperature was employed by welding the thermocouples on the specimen surface at the

Table 1 Chemical composition of the steel (wt. %)

C	Mn	Si	Cu	P	S	Nb	V	Ti	N	Fe
0.09	1.63	0.32	0.01	0.009	0.003	0.033	0.04	0.01	0.002	Rem.

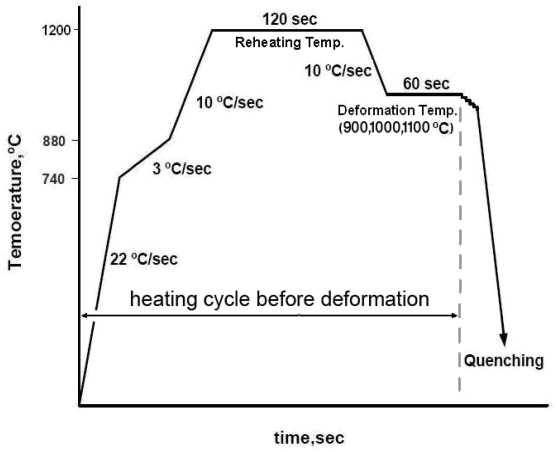

Fig. 2. The heating cycle before hot torsion test.

different points.

In order to investigate the influence of temperature gradient, developed in the gauge section of the samples during reheating, on austenite grain size distribution, the samples were austenized at 1200, 1150, 1100, 1050, and 1000°C and then quenched by helium gas with a cooling rate of more than 100°C.s^{-1}. Thermal etching was performed for revealing initial austenite grain boundaries according to reference [11]. Austenite grain size was calculated with mean linear intercept (or Heyn) metallographic procedure according to ASTM E11216 [12].

3. NUMERICAL AND EXPERIMENTAL RESULTS AND DISCUSSION

The time- temperature history of two points on the surface at the center and the end of gauge section for G1, G2, G3 and G4 specimens during reheating are shown in Fig. 3. For G2 and G4 the experimental data are also presented. The results in this figure indicate that by increasing the gauge length of the samples, temperatures of end sections of the samples deviate from those of the centre, hence from the expected heating cycle. In other words, by decreasing the gauge length, more homogenous temperature was obtained within the samples. The results shown in Fig. 3 indicate that the worst case is related to the sample G4 having a length longer than coil length of the furnace. It can be seen that the ends of gauge section in samples, G3, G4 and almost G2 were not only heated up to the planned deformation temperature but also even to the desired reheating temperature, i.e. 1200ºC. Consequently, a gradient of the initial austenite

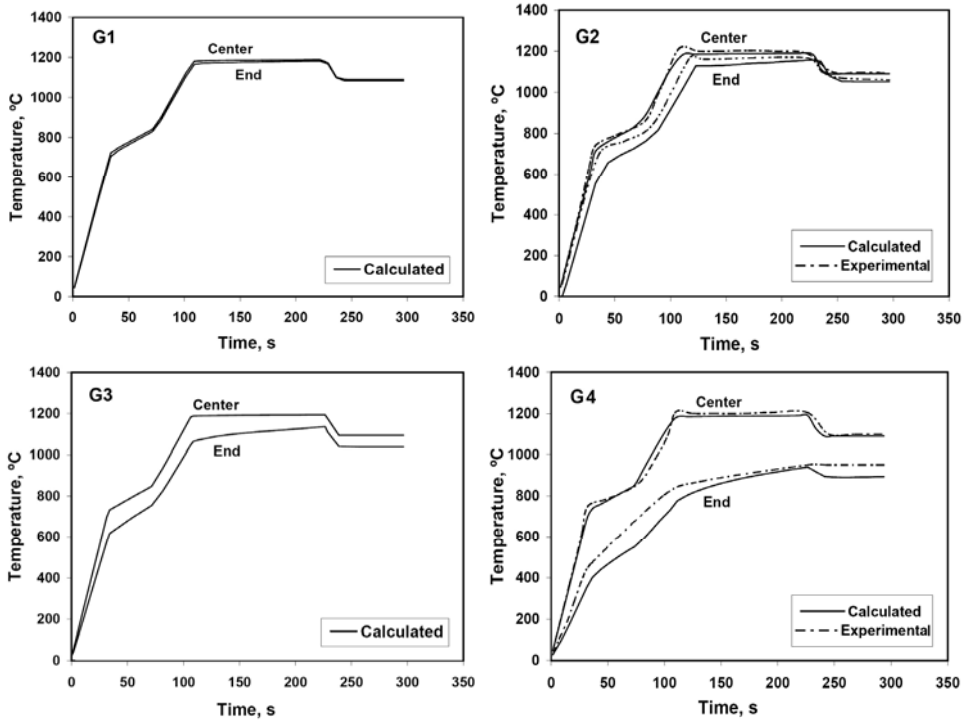

Fig. 3. The time- temperature history of two points on the surface of the gauge section of G1, G2, G3 and G4 specimens

grain size is predicted along the gauge section for these cases. In addition, solubility of microalloying elements (i.e. Ti, Nb and V) is expected to be different at the center and ends of the gauge because of the temperature gradient. Good agreement is observed between model prediction and the measured values for temperature. The average difference between prediction and measurement is within the tolerance limit of 25 ºC at reheat and deformation temperatures.

To study the austenite grain size of the steel at deferent points of the sample which experienced various temperature histories, grain size measurement performed and plotted in Fig.4. The results point out that the rate of grain growth was slow and had a normal trend in the temperature range of 1000-1175°C, but at temperatures higher than 1175°C, it became rapid and abnormal. At 1200°C and higher temperatures, an easier condition for the boundaries migration was provided. The grain boundary migration is known to be affected by particles, normally microalloying precipitates, within the grain boundaries. The higher the number of these particles, the lower will be the boundary migration. Therefore, at temperatures higher than 1175°C, some of the grain boundaries particles seemed to be dissolved within the boundaries which had a pinning effect for boundary migration according to reference [13]. So, this allowed the subsequent grain growth to happen. Indeed high temperature gradient in the gauge section of HTT samples could lead to different

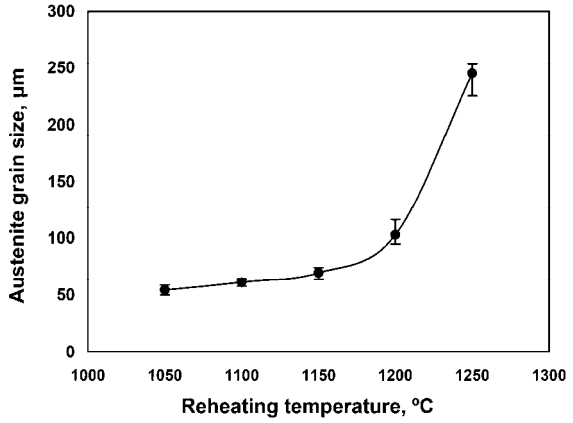

Fig. 4. Variation of austenite grain size with austenizing temperature

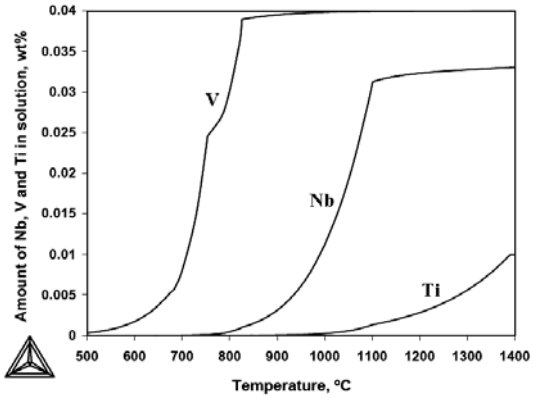

Fig. 5. Solubility of Nb, V and Ti at different temperatures

initial grain size at various region of the sample. This is significant for sample G4 as the high temperature difference between the center and both ends of gauge predicted, as shown in Fig.3.

A thermodynamic software Thermo-calc™ and its database, TCFE5, was used to predict solubility of microalloying elements of the steel under equilibrium conditions. Such solubility study is necessary for studying composition homogeneity within different geometries. Fig.5 illustrates that at temperatures higher than 1100°C, the entire amount of V in bulk (i.e. 0.04 wt. %) and nearly entire amount of Nb dissolve in the austenite but some of the enriched Ti precipitates are still stable. It seems reheating the samples at temperature 1200°C led to complete dissolution of V and Nb precipitates. One can conclude that small amount of grain growth at the temperatures lower than 1100°C was due to preventing effects of Nb and Ti particles which were still stable at this temperature. However, it was observed that at higher temperatures, i.e. above 1200°C where Nb precipitated completely and some of Ti precipitates dissolved in austenite, strong grain growth occurred.

Based on the calculated temperature distribution, it is expected that for the long samples, G3 and G4, at the ends of gauge section, solution of the chemical elements did not take place completely as at the center of sample. Consequently, a homogeneous composition within specimen can not be achieved before deformation. The significant temperature gradient developed in long samples not only resulted in non-uniform grain size, but also

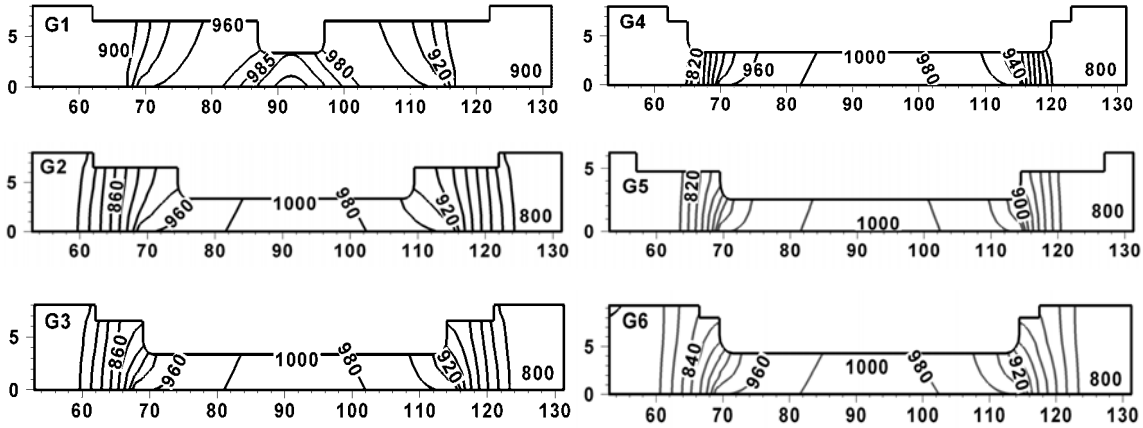

Fig. 6. Prediction of initial temperature distribution in G1, G2, G3, G4, G5, G6, after applying heating cycle and before deformation at 1000ºC

created composition profile of microalloying elements along the sample. As a result, more internal variables are needed to describe constitutive behavior of the material. A combination of non-uniform microstructure and localized temperature at the center makes the material more susceptible to flow localization during the test. Furthermore, this will introduce serious complexity and errors in deriving the constitutive parameters for the material.

Thermal solutions obtained by ANSYS are shown in Fig. 6 as the contour plots of temperature distribution for various geometries of HTT specimens after applying heating cycle (Fig.2) and before starting deformation at 1000ºC. The results display non uniform temperature along the axis of the specimens. This led to temperature gradients within the gauge part of the specimen. It can also be observed that specimens having longer gauge lengths, show greater thermal gradient. A maximum temperature difference of 160ºC between center and both ends of the gauge section can be seen for G4 specimen with a gauge length of 52mm. It should be noted that in practice the length of the induction coil of the furnace remains unchanged. For this analysis, an induction coil of 45mm long was assumed. Due to existence of a large air gap between coil and gauge surface, usually induction coil heats mostly the shoulders. The gauge section will be heated via heat transfer from the shoulder together with inducted heat from the coil.

It should be mentioned, the finite element calculations shown in Fig. 6, indicate that for the cases investigated, temperature variations in the radial direction were negligible (about 10ºC) within the gauge part of all specimens. It should also be mentioned that, because of the strain gradient from surface to center of the specimen, there is a gradient of heat generation in radial direction. This causes a normal non-uniform temperature across the cross section. However, heat loss from center to the surface is not the same.

Thermo-calc™ was also used to determine the possible equilibrium precipitates over a range of temperatures, particularly at deformation temperature range. This prediction showed three kinds of microalloying precipitates formed at different temperatures for the present steel. They were Ti, Nb and V enriched phases which most of them are complex precipitates. These microalloying elements react with both carbon

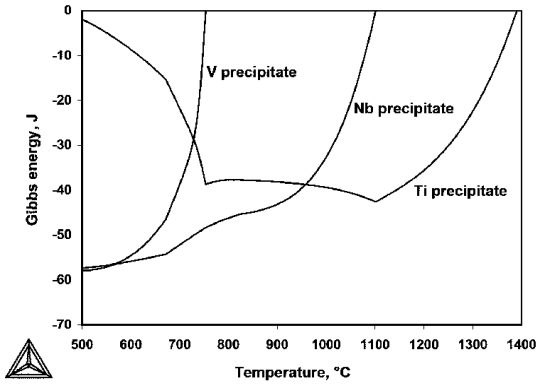

Fig.7. Gibbs energy of formation of Ti, Nb and V precipitates for X70 predicted by Thermo-calc™

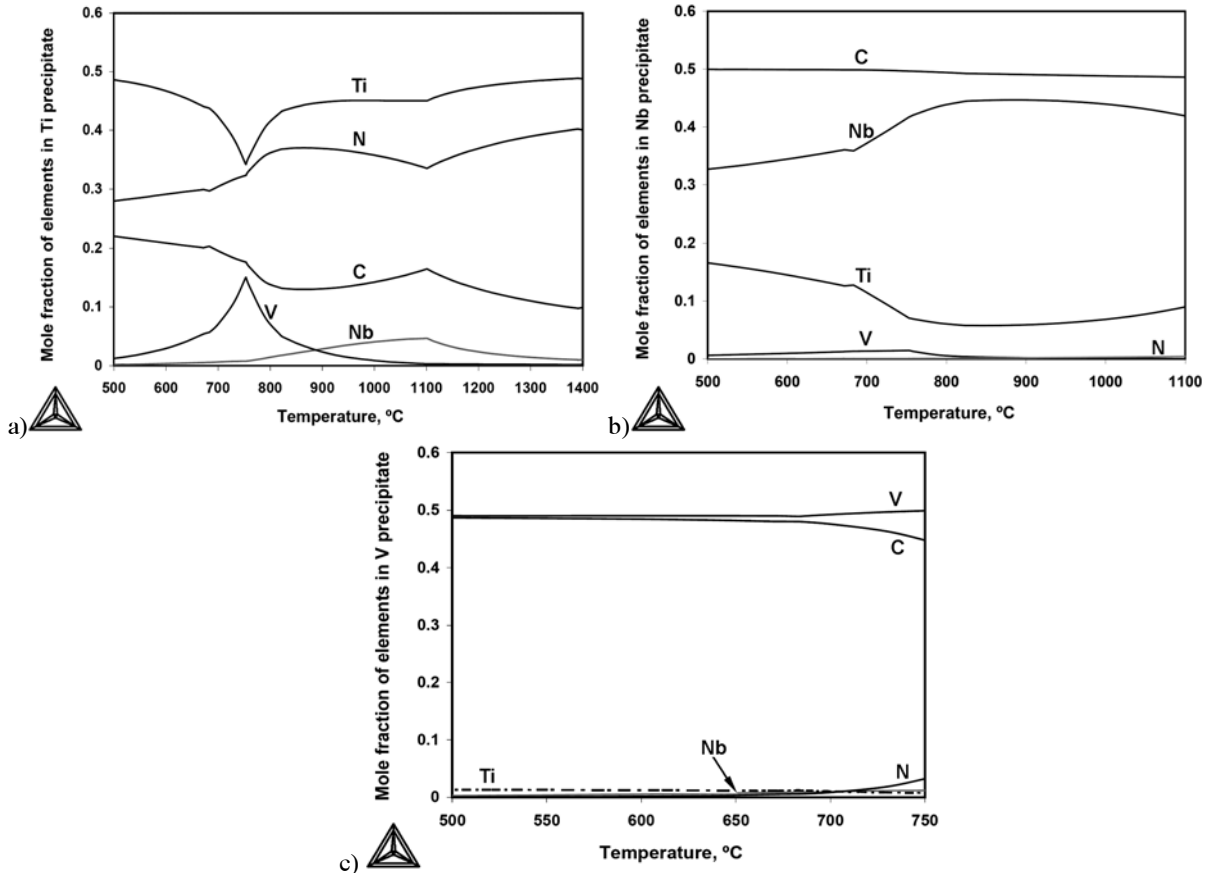

Fig. 8. Composition of a) Ti, b) Nb and c) V precipitates over temperature range predicted by Thermo-calc^{TM}

and nitrogen to form carbides, nitrides or carbonitrides. The Gibbs energy of formation of these precipitates is presented in Fig.7. The overall free energy change for precipitate formation consists of chemical free energy arising from the chemical super saturation of solutes and the interfacial energy spent on creation of the precipitate/matrix interface. It can be observed from Fig.7 that Ti, Nb and V enriched phases are expected to precipitate at around 1400°C, 1100°C and 750°C respectively.

Microchemistries of Ti, Nb and V precipitates as a function of temperature are illustrated in Fig. 8. Figure 8-a shows that the Ti precipitate was a carbonitride precipitate, (Ti,Nb)(C,N). As the temperature decreased from 1400°C to 1100°C the amount of Nb in the Ti precipitate increased as a solid solution. When Nb precipitated at temperature of 1100°C (Fig.7), the amount of Nb in the (Ti,Nb)(C,N) decreased. At lower temperatures than 900°C, Nb was replaced by V in the lattice of Ti precipitates until the V precipitates formed at temperature of 750°C (Fig.7). Study of composition of Nb precipitate in Fig.8-b shows that the precipitates exist as a complex carbide, namely (Nb,Ti)C precipitates. It is worth mentioning that the carbon content of Nb precipitates was constant over the temperature range used. In fact, the carbides and nitrides show extensive mutual solubility and the resulting solid solution can be described as a carbonitride [14].

Composition of V precipitates in Fig.8-c indicates that they are in form of VC. However, at the beginning of precipitation, a little amount of N existed in the precipitates which decreased by decreasing temperature. At temperatures higher than 1000°C, vanadium was completely soluble in austenite (Fig.5), but as temperature decreased from 1000°C to 750°C, solubility of vanadium decreased and it diffused into the Ti precipitates, to form complex precipitates of (Ti,V)(C,N).

The composition of microalloying precipitates may change over temperature range according to the solubility of these elements in the austenite.

Considering the fact the carbides and nitrides of Ti, Nb and V have similar FCC structures and have very similar lattice parameters, one could see that they may also form complex precipitates. Such complex precipitates have been reported in some experimental investigations [15-17].

Precipitation of microalloying elements occur at different temperatures and the amount of their precipitates varies over a temperature range. This is to say that precipitation may occur homogeneously only in the samples having short gauge length i.e. G1 and G2. Contour plots of temperature shown in Fig.6 can indicate precipitates distribution. It can be observed that the higher magnitude of differential temperature, the less is the amount of homogeneity. Inadequate dissolution of microalloying elements at soaking temperature which is significant for long samples would affect presence of present precipitates before deformation.

The result presented indicates that assumption of uniform temperature distribution in the gauge part of the specimen in previous works [18-20] may not be valid. It is well known the softening phenomena including recovery and recrystallization during hot deformation are influenced by microalloying elements [2, 4, 5, 14]. They might retard softening of material by either solute drag effect or pinning effect. So non uniform distribution of microalloying or precipitates along the sample could affect flow behavior of material at different points of the sample. As a result, the post processing of the test results become more complicated due to occurrence of flow localization. Therefore to trace an error encountered at the final test result, the proposed approach is required.

4. CONCLUSIONS

There exists an optimum geometry for a given experimental setup of HTT that leads to a minimum temperature difference in the gauge section of its specimen. The setup parameters include size of induction coil, thermal characteristics (conductivity, conductance, radiation view factor etc.) of grippers, capacity of furnace, reheating temperature. A number of FE thermal analyses for the test were performed to investigate the effect of geometry of the samples for a given heating cycle. Based on the numerical and experimental results, it can be concluded that:

1. The specimen geometry and the reheating cycle are the key parameters in obtaining uniform temperature distribution before HTT.
2. The initial microstructure features, i.e. initial austenite grain size and dissolution and precipitation of microalloying elements in the specimen, were both influenced by temperature distribution.
3. An optimum geometry and heating cycle was identified to minimize non homogenous initial austenite grain sizes, dissolution and precipitation of microalloying elements within the specimen.
4. For the fixed setup conditions, specimens G1 and G2 were proved to develop lowest temperature gradient in both radial and longitudinal directions of the gauge section.
5. Considering many possible combinations of the test setup, computer aided optimization of sample geometry and post processing of HTT is necessary for accurate results. The proposed optimization procedure can generally be used to predict temperature gradient along the gauge part of the specimen and microstructure features affected by it for other materials and reheating scenarios.

ACKNOWLEDGMENT

The corresponding author is grateful for the assistance of Arak University providing him a scholarship. The authors also acknowledge Sadid industrial group for the steel, and Mr. A. Abdolhosseini for doing some of the experimental tests.

REFERENCES

1. Samuel, F.H., Yue, S., Jonas, J.J. and Zbinden, B.A., (1989). "Modeling Testing of Flow Stress and Rolling Load of a Hot Strip Mill by Torsion." ISIJ International, 29, 878-886.
2. Bia, D.Q., Yue, S., Sun, W.P., Jonas, J.J., (1993). "Effect of Deformation Parameters

on the No-Recrystallization Temperature in Nb-Bearing Steels", Metallurgical Transactions A, Vol. 24A, 2151-2159.
3. Carsi, M., Lopez, V., Penalba, F., Ruano, O.A., (1996). "The strain rate as a factor influencing the hot forming simulation of medium carbon microalloyed steels", Materials Science and Engineering A, Vol. A216, 155-160.
4. Hodgson, P.D., L. X. Kong., Davies, C.H.J., (1999). "The prediction of the hot strength in steels with an integrated phenomenological and artificial neural network model", Journal of Materials Processing Technology, 87, 131-138.
5. QUISPE, S. F. M. a. A. (2001). "Improved Model for Static Recrystallization Kinetics of Hot Deformed Austenite in Low Alloy and Nb/V Microalloyed Steels." ISIJ International, 41, 174-781.
6. Kuc, D., Niewielski, G., and Cwajna, J. (2006). "Influence of deformation parameters and initial grain size on the microstructure of austenitic steels after hot-working processes." Materials Characterization, 56, 318–324.
7. Dieter, G., Howard, A., Kuhn, S. and Semiatin, L. (2003). Handbook of Workability and Process Design, ASM.
8. Bruno, J. C., and Rios, P. R., The Grain Size Distribution and the Detection of Abnormal Grain Growth of Austenite in an Eutectoid Steel Containing Niobium, Saipta Metallurgica et Materia, vol 32, No. 4, pp. 601-606, 1995.
9. Flores, O., Martinez, L. "Abnormal Grain Growth of Austenite in a V-Nb Microalloyed Steel", J. of Materials Science, Vol. 32, pp. 5985- 5991, 1997.
10. Oudin, A., Barnett, M.R. and Hodgson, P.D. Grain size effect on the warm deformation behavior of a Ti-IF steel, Materials Science and Engineering, 2004. A 367: p. 282-294.
11. Andres, C.G.d., Caballero, F.G., Capdevila, C. and San Martin D. Revealing austenite grain boundaries by thermal etching: advantages and disadvantages, Materials Characterization, vol. 49, pp. 121-127, 2003.
12. "Metallography; Nondestructive Testing", E112, ASTM standards, Vol. 03.03, ASTM, 1984.
13. Porter, D.A. and Easterling, K.E. Phase Transformations in Metals and Alloys, 2nd edn, 1992, CRC Press.
14. Gladman, T. The Physical Metallurgy of Microalloyed Steels, London: The Institute of Materials; 1997. p. 177.
15. Suzuki, K., Miyagawa, S., Saito, Y. and Shiotani, K. Effect of Microalloyed Nitride Forming of Carbonitride and High Temperature Cast Low Carbon Nb Containing Steel Elements Ductility Slab on of Precipitation Continuously, ISIJ International, Vol. 35, No. 1, pp. 34- 41, 1995.
16. Poths, R.M., Higginson, R.L. and Palmiere, E.J. Complex Precipitation Behavior in a Microalloyed Plate Steel, Scripta Materialia, Vol. 44, pp.147-151, 2000.
17. Craven, A.J., He, K., Garvie, L.A.J. and Baker, T.N. Complex Heterogeneous Precipitation in Titanium Microalloyed Al-Killed HSLA Steels-I (Ti,Nb(C,N), Acta mater., Vol. 48, pp. 3857-3868, 2000.
18. Zhou, M. and Clode, M.P. A finite element analysis for the least temperature rise in a hot torsion test specimen, Finite Elements in Analysis and Design, 31, 1-14. (1998).
19. Khoddam, S., Lam, Y. C. and Thomson, P. F. The effect of specimen geometry on the accuracy of the constitutive equation derived from the hot torsion test, steel research, 66 (No. 2), 45-49, (1995).
20. Njiwa, R.K., Metauer, G., Marchal, A. and Stebut, J.V. Effect of self heating on the torque vs. equivalent tensile strain plot in high temperature torsion of visco-plastic material, Journal of Materials Science, 36, 5659-5663, (2001).